Biomedicine & Pharmacotherapy 138 (2021) 111439

Contents lists available at ScienceDirect

Biomedicine & Pharmacotherapy

journal homepage: www.elsevier.com/locate/biopha

Curcumin suppresses the malignancy of non-small cell lung cancer by modulating the circ-PRKCA/miR-384/ITGB1 pathway

Xiaoqing Xu [a,1], Xinyue Zhang [b,1], Yang Zhang [c], Zhipeng Wang [a,*]

[a] Department of Clinical Oncology, The Affiliated Hospital of Shandong University of TCM, Jinan, Shandong, China
[b] Department of Respiratory Diseases, The First Clinical Medical College of Shandong University of TCM, Jinan, Shandong, China
[c] Department of Respiratory Diseases, The Affiliated Hospital of Shandong University of TCM, Jinan, Shandong, China

ARTICLE INFO

Keywords:
Curcumin
NSCLC
circ-PRKCA
miR-384
ITGB1

ABSTRACT

Background: Curcumin exerts a suppressive effect in tumor growth by acting as a modulator of multiple molecular targets. Circular RNA hsa_circ_0007580 (circ-PRKCA) accelerates the tumorigenesis of non-small cell lung cancer (NSCLC). However, whether curcumin can regulate circ-PRKCA to inhibit NSCLC progression is unclear.

Methods: Cell viability, colony formation, apoptosis, migration, and invasion were analyzed using Cell Counting Kit-8 (CCK-8), plate clone, flow cytometry, or transwell assay. Expression of circ-PRKCA, microRNA (miR)-384, and ITGB1 mRNA (integrin subunit beta 1) mRNA were detected by quantitative real-time polymerase chain reaction (qRT-PCR). Curcumin repressed NSCLC growth through regulating circ-PRKCA expression was validated by xenograft assay. The targeting relationship between circ-PRKCA or ITGB1 and miR-384 was verified by dual-luciferase reporter assay. The level of ITGB1 protein was measured by western blotting.

Results: Circ-PRKCA and ITGB1 expression were elevated in NSCLC tissues and cells, but miR-384 had an opposing tendency. After curcumin treatment, the expression tendency of circ-PRKCA, miR-384, and ITGB1 in NSCLC cells was overturned. Furthermore, curcumin impeded viability, colony formation, migration, invasion, and accelerated apoptosis of NSCLC cells, but these impacts were partially reversed by circ-PRKCA elevation, miR-384 downregulation, or ITGB1 overexpression. Also, the inhibitory effect of curcumin on xenograft tumor was further enhanced after circ-PRKCA knockdown. Notably, circ-PRKCA regulated ITGB1 expression through sponging miR-384 in curcumin-treated NSCLC cells.

Conclusions: Curcumin inhibited NSCLC growth through downregulating circ-PRKCA, which regulated ITGB1 expression by adsorbing miR-384. This study provided a new mechanism to understand how curcumin inhibited the progression of NSCLC.

1. Introduction

The mortality and incidence of lung cancer rank first among all malignant tumors in the world, and 80%–85% of patients are non-small cell lung cancer (NSCLC) [1,2]. Although medical management has made great progress, the prognosis of NSCLC patients is still not ideal [3,4]. Thus, there is an urgent need to develop new treatment options to improve the prognosis of NSCLC.

Curcumin, a traditional herbal medicine, is discovered in *Curcuma longa*. It is a polyphenol and has many activities, including controlling diabetes, improving brain function, oxidation, anti-inflammatory, anti-tumor, and so on [5]. It has been reported that curcumin plays an important role in various cell signal transduction by acting as a modulator of multiple molecular targets [6]. Also, curcumin plays a repressive role in the advancement of NSCLC. Zhang et al. manifested that curcumin synergistically constrained cell malignancy via controlling EGFR and TLR4/MyD88 pathways in NSCLC cells [7]. Furthermore, curcumin played an anti-tumor activity in NSCLC cells through inactivating the Wnt/β-catenin [8] or PI3K/Akt/mTOR [9] pathway. At present, the mechanism by which curcumin inhibits the malignancy of NSCLC cells is still unclear.

Circular RNAs (circRNAs), a group of endogenous RNAs different

* Correspondence to: Department of Clinical Oncology, The Affiliated Hospital of Shandong University of TCM, 16369# Jingshi Road, Jinan 250014, Shandong, China.
E-mail address: jnxuxiaoqing@126.com (Z. Wang).
[1] Xiaoqing Xu and Xinyue Zhang contribute to this work equally as co-first authors.

https://doi.org/10.1016/j.biopha.2021.111439
Received 16 December 2020; Received in revised form 23 February 2021; Accepted 23 February 2021
Available online 6 March 2021

from linear RNAs, are characterized by covalently closed-loop structures lacking poly-adenylated tails. There are four types of circRNAs, including intergenic circRNAs, intron circRNAs, exon circRNAs, and exon-intron circRNAs [11]. Exon circRNAs, which are produced by pre-mRNA through back-splicing, account for more than 80% of all types of circRNAs [12]. Based on the ceRNA hypothesis, circRNAs can bind to microRNAs (miRs) through miR response elements, thus sequestering miRs and regulating downstream targets of miRs [13]. Emerging evidence has manifested that the abnormal expression of some circRNAs is implicated in the advancement of human diseases, including cancer [14,15]. For example, circRNA circ-0072995 upregulation accelerated epithelial ovarian cancer development via modulating the miR-147a/CDK6 axis [16]. CircRNA hsa_circ_0007580 (circ-PRKCA) is derived from the PRKCA (protein kinase C alpha) gene. Chen et al. found that circ-PRKCA downregulation impeded the tumorigenesis of NSCLC by adsorbing miR-545–3p [17]. A recent study indicated that curcumin decreased radioresistance through modulating the circRNA/miR/mRNA network in nasopharyngeal carcinoma [10]. Nevertheless, it is unclear whether curcumin can restrain NSCLC progression by changing the expression of circ-PRKCA.

In the present study, we verified that curcumin repressed circ-PRKCA expression in NSCLC cells. Importantly, curcumin repressed the malignancy of NSCLC cells through regulating the circ-PRKCA/miR-384/ITGB1 (integrin subunit beta 1) pathway.

2. Materials and methods

2.1. Tissue specimens

29 paired NSCLC tissue specimens and adjacent normal tissues were obtained from The Affiliated Hospital of Shandong University of TCM. None of the recruited patients had received chemotherapy or other treatments before surgery. All excised specimens were kept at − 80 °C until use. The project was approved by the Ethics Committee of The Affiliated Hospital of Shandong University of TCM, and all registered NSCLC patients had provided written consents.

2.2. Cell culture and treatment

NSCLC cells (H1650, H1299, H460, and A549), human bronchial epithelial cell line (16HBE), and 293T cells were purchased from Procell (Wuhan, China) and cultured in Ham's F-12 K medium (Thermo Fisher Scientific, Waltham, MA, USA) (for A549 cells) or Roswell Park Memorial Institute-1640 (RPMI-1640) medium (Procell, cat. no. PM150110) (for H1650, H1299, H460, 16HBE, and 293T cells) supplemented with 10% fetal bovine serum (FBS) (Procell, cat. no. 164210) and 1% penicillin/streptomycin (Procell, cat. no. PB180120). The growth of all cells was kept at 37 °C under 5% CO_2.

To explore the influence of curcumin (Sigma, St Louis, MO, USA) on the malignancy of NSCLC cells, H460 and A549 cells were grown in their respective media containing different concentrations of curcumin (0, 10, 20, 40 μM) for 24 h. For function analysis, H460 and A549 cells were cultured in their respective media containing 20 μM curcumin for 24 h.

2.3. Transfection of plasmids and oligonucleotides

Transient transfection was executed using Lipofectamine 3000 reagent (Thermo Fisher Scientific). The pCD5-ciR-circ-PRKCA (circ-PRKCA) and pcDNA-ITGB1 (ITGB1) vectors were constructed using pCD5-ciR vectors (Vector) (Geneseed, Guangzhou, China) or pcDNA (pcDNA) vectors (Thermo Fisher Scientific). Short hairpin (sh) RNA targeting circ-PRKCA (sh-circ-PRKCA) and matching negative control (NC) (sh-NC), small interfering (si) RNA against circ-PRKCA (si-circ-PRKCA) and matching NC (si-NC), miR-384 mimic (miR-384) and its NC mimic (miR-NC), and miR-384 inhibitor (anti-miR-384) and its NC mimic (anti-miR-NC) were synthesized by GenePharma (Shanghai, China).

2.4. Cell viability assessment

Cell Counting Kit-8 (CCK-8) (Solarbio, Beijing, China) was employed to test the viability of 16HBE and NSCLC cells. Briefly, these cells were seeded into 96-well plates and grown for 24 h. Then, these cells were treated with curcumin for 24 h, and phosphate buffer saline (PBS) (Thermo Fisher Scientific) was used as a control. Thereafter, CCK-8 solution (10 μL) was added to each well and the optical density (OD) value at 450 nm was assessed using a Microplate Reader (Bio-Rad, Hercules, CA, USA) after incubation for 2 h.

2.5. Plate clone assay

In brief, H460 and A549 cells were suspended in their respective media containing 0.3% ager (Sigma) and 20 μM curcumin. After culture for 24 h, the cells (1.0×10^3) were plated into 6-well plates, which were preloaded with a thin layer of 0.6% agar (Sigma). 10 days later, the cells were stained with 0.1% crystal violet solution (Sigma). The clones > 50 cells were counted using a Nikon Eclipse E600 microscope (Nikon Instruments, Melville, NY, USA).

2.6. Cell apoptosis assessment

After transfection for 24 h, H460 and A549 cells were treated with 20 μM curcumin for 24 h. Cell apoptosis was evaluated using an Annexin V-fluorescein isothiocyanate (FITC)/propidium iodide (PI) apoptosis detection kit (Becton Dickinson, San Jose, CA, USA) in accordance with manufacturer's instructions. In short, the cells were digested with trypsin (Sigma) to form a single cell. Then, the cells (1.0×10^6) were resuspended in binding buffer (1 mL, 1 ×). Subsequently, the cells (1.0×10^5) were incubated with Annexin V-FITC (5 μL) for 10 min and then stained with PI (5 μL) for 5 min. FACS Calibur Flow Cytometer (Becton Dickinson) with a CellQuest software program (Becton Dickinson) was used to determine dead cells, live cells, early apoptotic cells, and late apoptotic cells.

2.7. Migration and invasion assessment

For migration assay, H460 and A549 cells (1×10^5 cells/well) in 200 μL medium containing 1% bovine serum albumin (Sigma) and 20 μM curcumin were tiled to the upper chamber of the 24-well transwell chamber (Corning, Corning, NY, USA). Also, the lower chamber was added with 600 μL medium containing 10% FBS. 24 h later, the migrating cells were fixed by 4% paraformaldehyde (Sigma) and stained with 0.25% crystal violet (Sigma). The number of the migrating cells was figured using a Nikon Eclipse E600 microscope (Nikon Instruments) at 100 × magnification. The steps of the invasion assay and the migration assay were the same, the only difference was that the upper chamber of the transwell chamber used in the invasion assay was precoated with Matrigel matrix (Corning).

2.8. Quantitative real-time polymerase chain reaction (qRT-PCR)

Total RNA extraction was conducted with the miRNeasy Mini Kit (Qiagen, Hilden, Germany). The quality of the extracted RNA was analyzed using the SmartSpec Plus Spectrophotometer (Bio-Rad, Hercules, CA, USA) (A260/A280 nm) and agarose gel (Biowest, Kansas, MO, USA) electrophoresis (1%). Total RNA was reverse-transcribed using a reverse transcription kit (Promega, Madison, WI, USA) or miRNA first-stand cDNA synthesis kit (GeneCopoeia, Guangzhou, China). QRT-PCR was conducted using the SYBR Green PCR Master Mix (Applied Biosystems, Foster City, CA, USA) in the ABI7500 system (Applied Biosystems). All primer sequences were listed as follows: glyceraldehyde-3-phosphate dehydrogenase (GAPDH) (forward (F): 5′-

GACTCCACTCACGGCAAATTCA-3′; reverse (R): 5′-TCGCTCCTGGAAGATGGTGAT-3′), circ-PRKCA (F: 5′-TATCGCCCCAGAGAAAGCCA-3′; R: 5′-CGGTCAAGGTTGTTGGAAGGT-3′), PRKCA (F: 5′-GCCTATGGCGTCCTGTTGTATG-3′; R: 5′-GAAACAGCCTCCTTGGACAAGG-3′),

miR-384 (F: 5′-ATTCCTAGAAATTGTTCATA-3′; R: 5′-GAACATGTCTGCGTATCTC-3′), ITGB1 (F: 5′-GGATTCTCCAGAAGGTGGTTTCG-3′; R: 5′-TGCCACCAAGTTTCCCATCTCC-3′), and U6 small nuclear RNA (U6) (F: 5′-GCTCGCTTCGGCAGCACA-3′; R: 5′-GAGGTATTCGCACCAGAGGA-3′). Relative expression was figured by the $2^{-\Delta\Delta Ct}$ method and normalized to GAPDH or U6.

2.9. RNase R treatment

RNase R treatment was performed to verify the circular form of circ-PRKCA. In short, total RNA from H460 and A549 cells was digested with DEPC-treated water (Thermo Fisher Scientific) or RNase R (Epicentre Technologies, Madison, WI, USA) at 37°C. 30 min later, the levels of circ-PRKCA and PRKCA mRNA were tested using qRT-PCR.

2.10. Subcellular fractionation location

The isolation of cytoplasmic RNA and nuclear RNA was executed with the PARIS™ Kit (Thermo Fisher Scientific) based on the previous description [18]. QRT-PCR was carried out to evaluate circ-PRKCA expression in the cytoplasmic RNA and nuclear RNA. U6 is mostly distributed in the nucleus, while GAPDH is mostly distributed in the cytoplasm [1]. Thus, U6 and GAPDH were utilized as positive control for nuclear and cytoplasmic fractions, respectively.

2.11. Construction of stable A549 cell line

The pLKO.1-sh-NC and pLKO.1-sh-circ-PRKCA were constructed using the pLKO.1 vectors (Sigma). 293 T cells were transfected with pLKO.1-sh-NC or pLKO.1-sh-circ-PRKCA using polyethylenimine (Ployscienes, Warrington, PA, USA). After transduction with lentiviral vectors (from the supernatant of 293T cells), A549 cells were selected with puromycin (5 μg/mL, Solarbio).

2.12. Xenograft assay

The experiment was approved by the Animal Ethics Committee of The Affiliated Hospital of Shandong University of TCM. 32 BALB/c nude mice (4-week-old) were bought from Vital River Laboratory (Beijing, China). The mice were randomly divided into 4 groups and processed as follows: (1) Mice were subcutaneously injected with A549 cells carrying sh-NC (4×10^6/0.2 mL PBS); (2) Mice were subcutaneously injected with A549 cells carrying sh-circ-PRKCA (4×10^6/0.2 mL PBS); (3) Mice were given curcumin (50 mg/kg) orally; (4) Mice were subcutaneously injected with A549 cells carrying sh-circ-PRKCA (4×10^6/0.2 mL PBS) and administered curcumin (50 mg/kg) orally. Mice were given curcumin (50 mg/kg) every 3 days from the seventh day [19]. Tumor volume was measured every 3 days and calculated in accordance with the following equation: Volume = (length × width^2)/2. 22 days later, all mice were killed by cervical dislocation under anesthesia. Thereafter, all tumor tissues were excised, weighed, and then stored frozen at − 80 °C for subsequent analysis.

2.13. Dual-luciferase reporter assay

The sequence of circ-PRKCA or ITGB1 complementary to miR-384 was predicted using the circInteractome (https://circinteractome.nia.nih.gov/api/v2/mirnasearch?circular_rna_query=hsa_circ_0007580&mirna_query=hsa-miR-384&submit=miRNA+Target+Search) or starBase (http://starbase.sysu.edu.cn/agoClipRNA.php?source=mRNA&flag=target&clade=mammal&genome=human&assembly=hg19&miRNA=hsa-miR-384&clipNum=1&deNum=0&panNum=0&proNum=1&program=&target=ITGB1#modal) databases. For luciferase reporter construction, the wild type (WT) sequences of circ-PRKCA (WT-circ-PRKCA) and 3′ untranslated regions (UTR) of ITGB1 (ITGB1 3′UTR-WT) and their mutant (MUT) sequences (MUT-circ-PRKCA and ITGB1 3′UTR-MUT) were synthesized and inserted into the pMIR-REPORT vectors (Applied Biosystems), respectively. H460 and A549 cells were cotransfected with a luciferase reporter plasmid (100 ng), pRL-SV40 (10 ng), and miR-NC or miR-384 (50 nM) using Lipofectamine 3000 reagent (Thermo Fisher Scientific). The luciferase activities in cell lysates were analyzed using the luciferase reporter assay kit (Promega) in a TD20/20 Luminometer (Turner Biosystems, Sunnyvale, CA, USA).

2.14. Western blotting

Total protein isolation was performed using the RIPA (Radio-Immunoprecipitation Assay) buffer (Sigma). The concentration of the extracted total protein was analyzed using a BCA assay (Pierce, Rockford, IL, USA). Total protein was isolated by sodium dodecyl sulfate-polyacrylamide gel electrophoresis. Thereafter, the isolated proteins were transferred to polyvinylidene fluoride (PVDF) membranes (Sigma) and blocked in tris buffered saline tween buffer containing 5% skim milk. The membranes were incubated with anti-ITGB1 (#14-0299-80, 1:1000, Thermo Fisher Scientific) or anti-GAPDH (#MA5-15738-D800, 1:1000, Thermo Fisher Scientific) antibodies. Then, the membranes were incubated with a goat anti-mouse IgG secondary antibody (#31430, 1:10000, Thermo Fisher Scientific). The blots were detected by enhanced chemiluminescence (ECL) substrates (Thermo Fisher Scientific). GAPDH was deemed as a loading control.

2.15. Statistical analysis

All experiments in vitro were repeated 3 times. All data were analyzed by GraphPad Prism 7.0 (Graph-Pad Software, La Jolla, CA) and were presented as the mean ± standard deviation. The difference between NSCLC tissues and adjacent normal tissues was evaluated by paired Student's *t*-test. The difference between 2 groups was detected by unpaired Student's *t*-test. The differences among 3 or more groups were analyzed using one-way variance analysis (ANOVA) followed by Turkey's post hoc test. The correlation between circ-PRKCA or ITGB1 and miR-384 in NSCLC tissues was determined by Pearson's correlation analysis. Statistical significance was accepted when $P < 0.05$.

3. Results

3.1. Curcumin constrained the malignancy of NSCLC cells

To validate the impact of curcumin on the malignancy of NSCLC cells, we first evaluated the viability of NSCLC cells under curcumin treatment. CCK-8 assay exhibited that curcumin treatment did not change the viability of 16HBE cells, but it reduced the viability of NSCLC cells (H460 and A549) in a dose-dependent manner (Fig. 1A-C). Plate clone assay manifested that the cloning ability of H460 and A549 cells was gradually decreased with the increase of curcumin (Fig. 1D). Flow cytometry assay presented that curcumin treatment accelerated the apoptosis of H460 and A549 cells in a dose-dependent manner (Fig. 1E). Compared with the control group, the number of migrating and invading H460 and A549 cells was gradually reduced as the curcumin dose increased in transwell assay (Fig. 1F and G). These results indicated that curcumin curbed the malignant behaviors of NSCLC cells in a dose-dependent manner.

3.2. Circ-PRKCA was highly expressed in NSCLC tissues and cells

Previous research uncovered that circ-PRKCA expression was upregulated in NSCLC tissues [17]. To verify the differential expression of circ-PRKCA in NSCLC, we detected circ-PRKCA expression in 29 paired

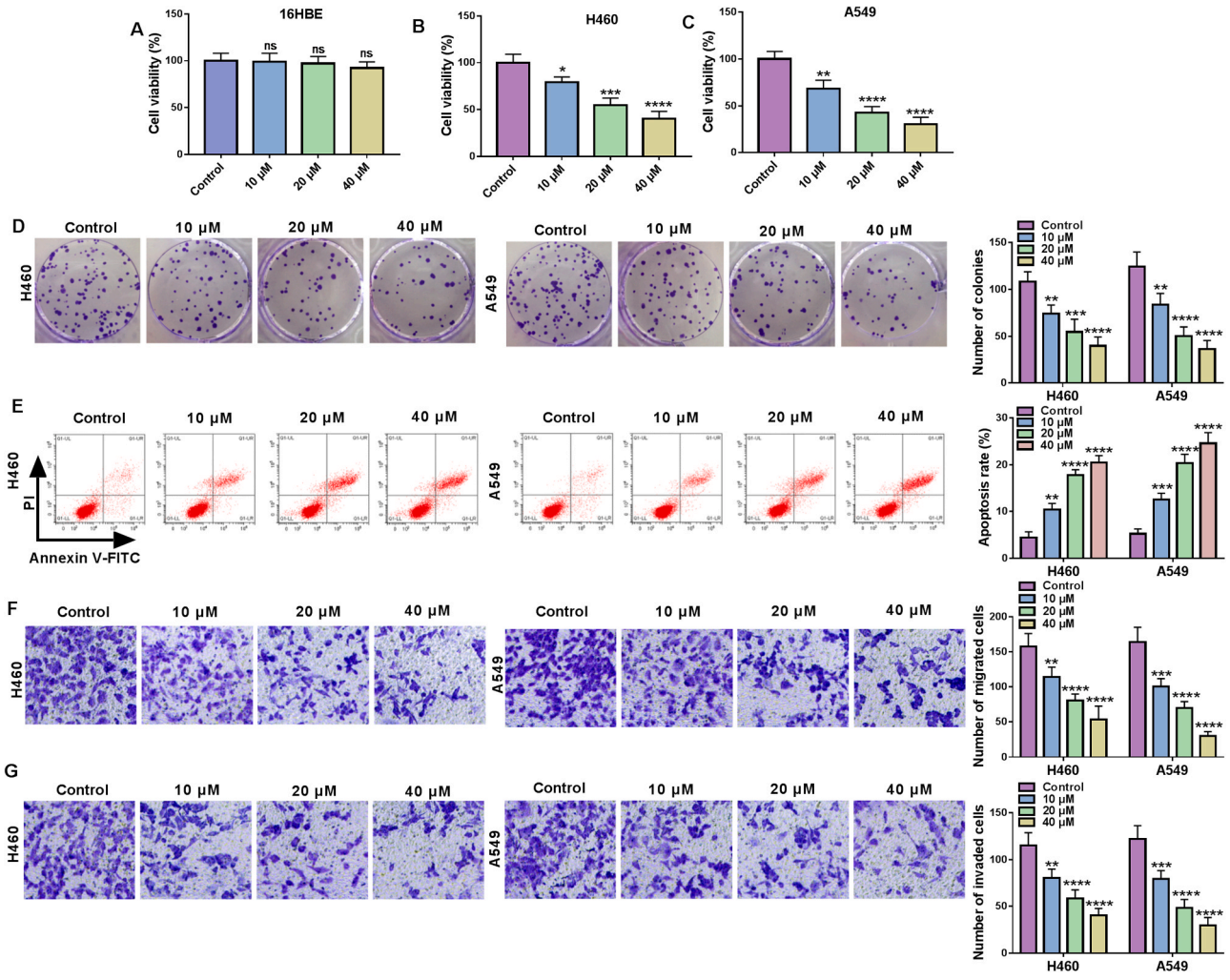

Fig. 1. Curcumin played a repressive influence on the malignancy of NSCLC cells. (A) Analysis of the viability of 16HBE cells treated with curcumin at different concentrations (0, 10, 20, 40 μM) by CCK-8 assay. (B-D) Assessment of viability and colony formation of H460 and A549 cells treated with curcumin at different concentrations (0, 10, 20, 40 μM) by CCK-8 and plate clone assays. (E) The apoptosis of H460 and A549 cells treated with different doses of curcumin (0, 10, 20, 40 μM) was assessed by flow cytometry assay. (F and G) The migration and invasion of H460 and A549 cells under curcumin treatment (0, 10, 20, 40 μM) were analyzed by using transwell assays. $^{*}P < 0.05$, $^{**}P < 0.01$, $^{***}P < 0.001$, and $^{****}P < 0.0001$.

NSCLC tissues and adjacent normal tissues. QRT-PCR showed that circ-PRKCA expression was higher in NSCLC tissues relative to adjacent normal tissues (Fig. 2A). Consistently, circ-PRKCA was highly expressed in NSCLC cells (H1650, H1299, H460, and A549) than that in 16HBE cells, especially in H460 and A549 cells (Fig. 2B). Exonuclease RNase R can degrade almost all linear RNA molecules from the 3′-5′ direction, but it is not easy to digest circular RNA molecules. Thus, we validated the circular structure of circ-PRKCA through RNase R treatment. As exhibited in Fig. 2C and D, circ-PRKCA expression was not affected after RNase R treatment in contrast to the mock group, whereas the level of linear PRKCA was overtly lower, illustrating circ-PRKCA had a circular structure. Furthermore, we observed that circ-PRKCA was predominantly localized in the cytoplasm of H460 and A549 cells, suggesting that circ-PRKCA might play a role in post-transcriptional regulation (Fig. 2E and F). Collectively, these results indicated that circ-PRKCA was upregulated in NSCLC and is predominantly localized in the cytoplasm.

3.3. Overexpression of circ-PRKCA reversed the inhibitory effect of curcumin treatment on the malignancy of NSCLC cells

To explore the involvement of circ-PRKCA and curcumin in NSCLC, we detected circ-PRKCA expression in H460 and A549 cells under curcumin treatment. As presented in Fig. 3A, circ-PRKCA expression was decreased in H460 and A549 cells with the increase of curcumin, but circ-PRKCA expression was not significantly different between 20 μM and 40 μM. Thus, 20 μM curcumin was used for function analysis. The overexpression efficiency of circ-PRKCA was exhibited in Fig. 3B. Furthermore, the downregulation of circ-PRKCA in H460 and A549 cells under curcumin treatment was partially restored after circ-PRKCA elevation (Fig. 3C). Also, circ-PRKCA overexpression overturned the inhibitory influence of curcumin on the viability and colony formation of H460 and A549 cells (Fig. 3D and E). Moreover, the elevation of apoptosis of H460 and A549 cells under curcumin treatment was abolished after circ-PRKCA overexpression (Fig. 3F). In addition, the inhibition of migration and invasion of H460 and A549 cells caused by curcumin treatment was reversed by forcing circ-PRKCA expression (Fig. 3G and H). Together, these data manifested that curcumin repressed the malignancy of NSCLC cells via downregulating circ-PRKCA.

3.4. Circ-PRKCA silencing enhanced the repressive influence of curcumin on xenograft tumor growth

Based on the above results, we further validated that curcumin modulated the malignancy of NSCLC cells through circ-PRKCA by xenograft assay. The results exhibited that circ-PRKCA was

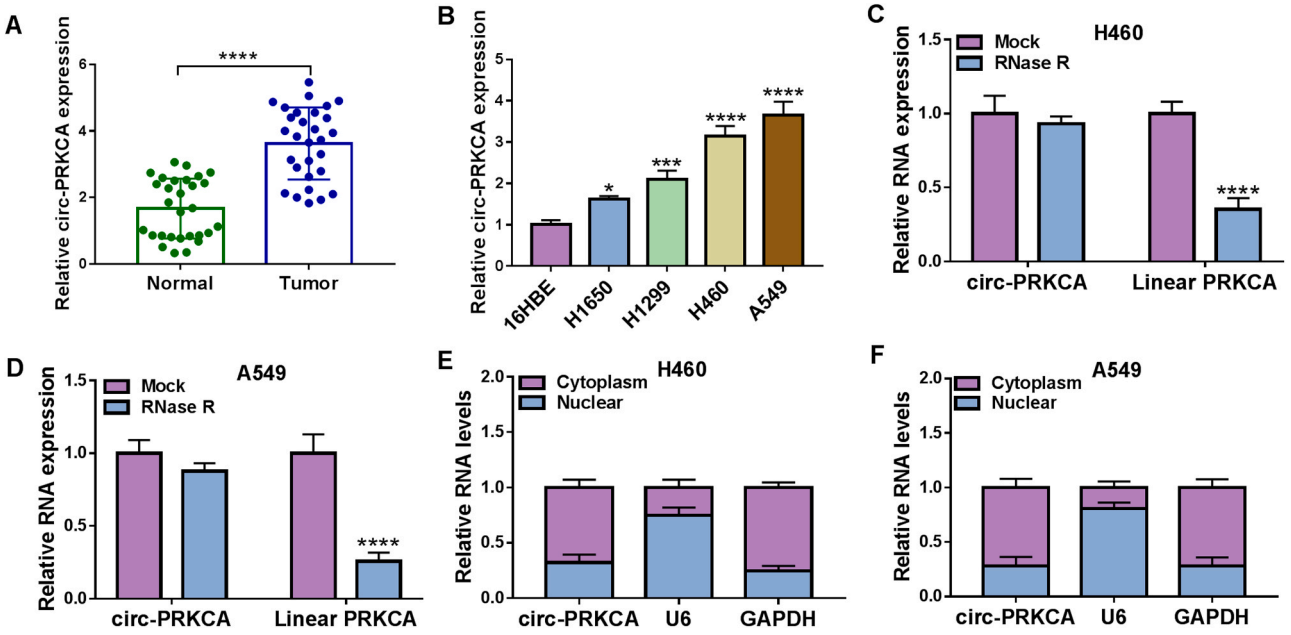

Fig. 2. Circ-PRKCA was upregulated in NSCLC. (A) Analysis of circ-PRKCA expression in 29 paired NSCLC tissues and adjacent normal tissues by qRT-PCR. (B) Analysis of circ-PRKCA expression in NSCLC cells (H1650, H1299, H460, and A549) and 16HBE cells by qRT-PCR. (C and D) RNase R treatment was performed to verify the circular structure of circ-PRKCA. (E and F) Identification of circ-PRKCA localized in the cytoplasm or nuclear of H460 and A549 cells by qRT-PCR. $^{*}P < 0.05$, $^{***}P < 0.001$, and $^{****}P < 0.0001$.

downregulated in A549 cells carrying with lentivirus-mediated sh-circ-PRKCA relative to the control group (Fig. 4A). Moreover, both circ-PRKCA inhibition and curcumin treatment reduced tumor volume and weight compared to the sh-NC group, whereas curcumin treatment further decreased tumor volume and weight in the sh-circ-PRKCA group (Fig. 4B and C). Also, circ-PRKCA expression was downregulated in the sh-circ-PRKCA and curcumin groups relative to the sh-NC group, but circ-PRKCA expression was further reduced in the sh-circ-PRKCA group treated with curcumin (Fig. 4D). These findings indicated that curcumin inhibited xenograft tumor growth through decreasing circ-PRKCA expression.

3.5. Circ-PRKCA was validated as a sponge for miR-384 in NSCLC cells

Given that circ-PRKCA was mainly located in the cytoplasm, we further investigated the regulatory mechanism of circ-PRKCA in NSCLC progression. After performing online bioinformatics prediction (circactactactome), we screened 6 miRs (miR-1299, miR-153, miR-188-3p, miR-330-5p, miR-598, and miR-384) that have inhibitory effects in non-small cell lung cancer for analysis. Also, circ-PRKCA silencing markedly elevated the levels of 4 miRs (miR-1299, miR-188-3p, miR-330-5p and miR-384) in A549 cells, especially miR-384 (Supplementary Fig. 1). To verify the involvement of miR-384 and curcumin in the malignancy of

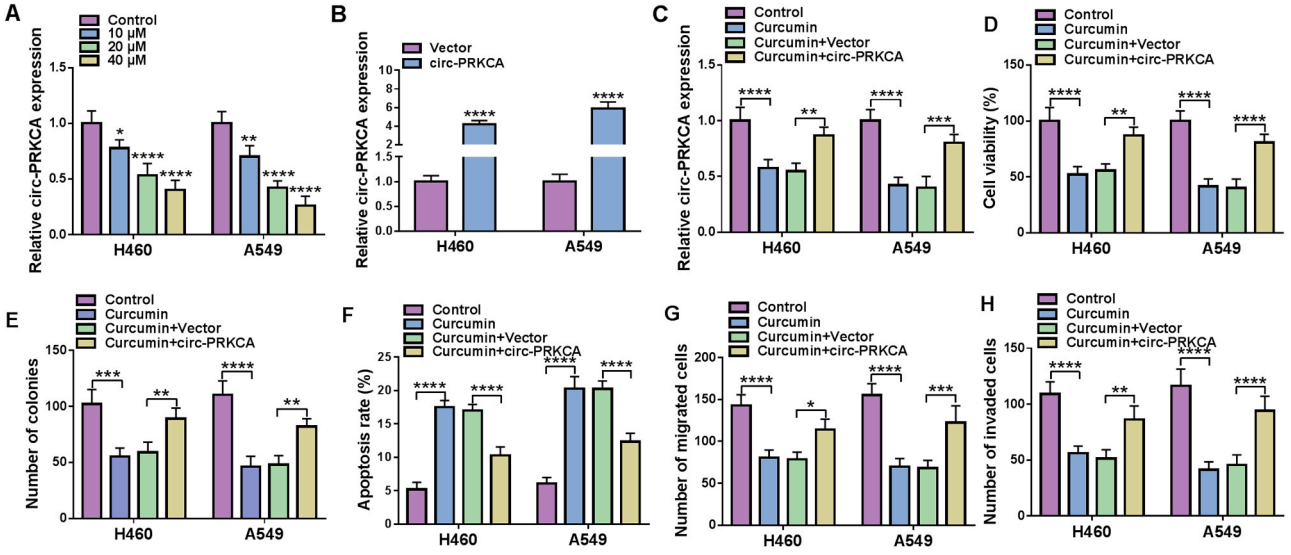

Fig. 3. Curcumin regulated the malignancy of NSCLC cells through circ-PRKCA. (A) Analysis of the expression of circ-PRKCA in H460 and A549 cells treated with curcumin at different concentrations (0, 10, 20, 40 μM) by qRT-PCR. (B) Overexpression efficiency of circ-PRKCA in H460 and A549 cells was verified by qRT-PCR. (C-H) After Vector or circ-PRKCA transfection, H460 and A549 cells were treated with 20 μM curcumin. (C) Assessment of the expression of circ-PRKCA in H460 and A549 cells under curcumin treatment by qRT-PCR. (D-H) Analysis of the viability, colony formation, apoptosis, migration, and invasion of H460 and A549 cells under curcumin treatment by CCK-8, plate clone, flow cytometry, and transwell assays. $^{*}P < 0.05$, $^{**}P < 0.01$, $^{***}P < 0.001$, and $^{****}P < 0.0001$.

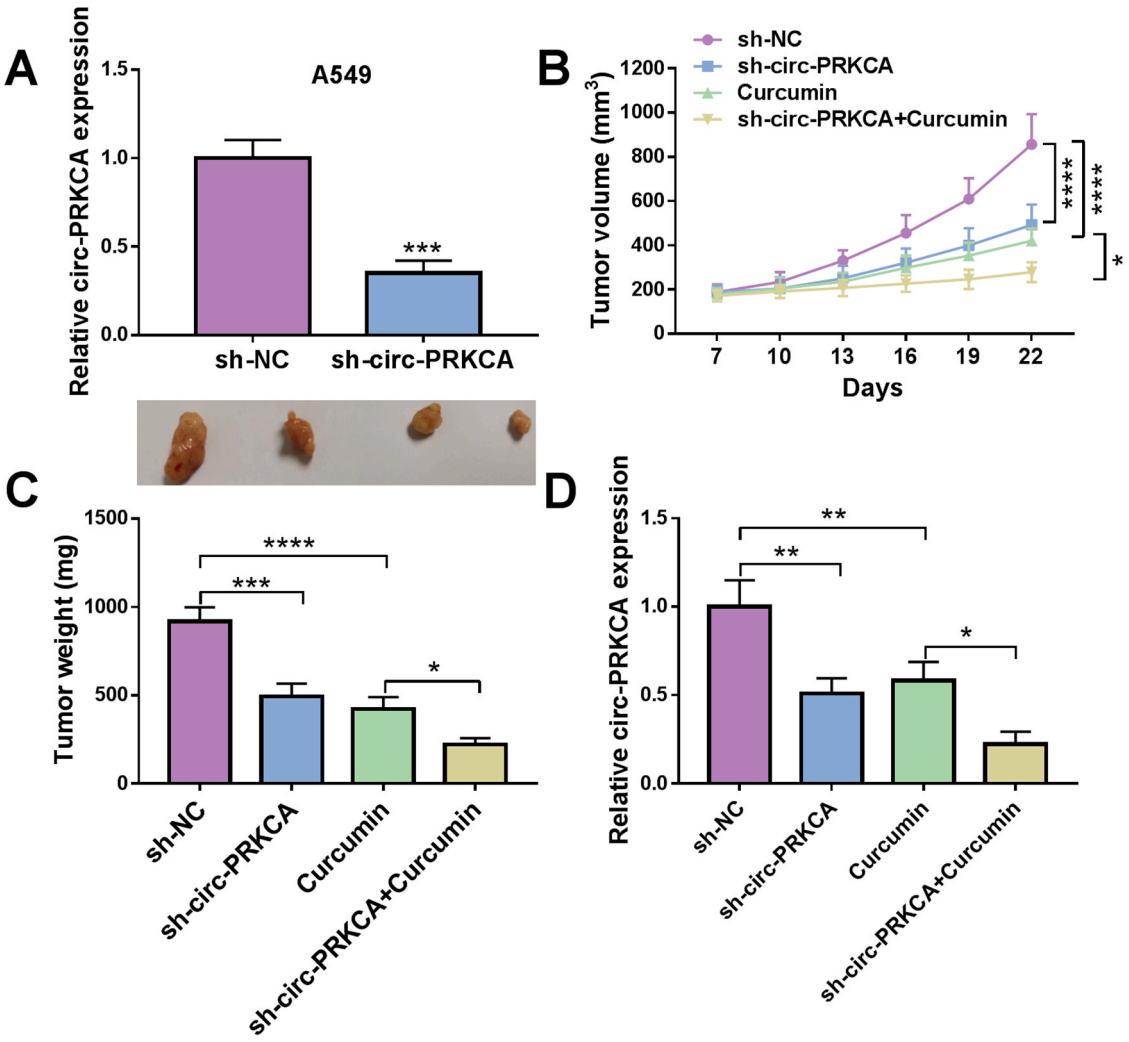

Fig. 4. Curcumin inhibited xenograft tumor growth through circ-PRKCA. (A) QRT-PCR revealed the expression of circ-PRKCA in A549 cells stably transfected with sh-circ-PRKCA or sh-NC. (B) The growth curves of xenograft tumor in the sh-NC, sh-circ-PRKCA, curcumin, and sh-circ-PRKCA+curcumin groups. (C) Xenograft tumor weight in the sh-NC, sh-circ-PRKCA, curcumin, and sh-circ-PRKCA+curcumin groups. (D) QRT-PCR presented the expression of circ-PRKCA in mice tumor tissues in the sh-NC, sh-circ-PRKCA, curcumin, and sh-circ-PRKCA+curcumin groups. $^{*}P < 0.05$, $^{**}P < 0.01$, $^{***}P < 0.001$, and $^{****}P < 0.0001$.

NSCLC cells, we detected the expression of miR-384 in H460 and A549 under curcumin treatment. The results exhibited that miR-384 expression was elevated in curcumin-treated H460 and A549 cells in a dose-dependent manner (Fig. 5A). Predicted binding sites between circ-PRKCA and miR-384 were exhibited in Fig. 5B. Dual-luciferase reporter assay exhibited that miR-384 mimic reduced the luciferase activity of the WT-circ-PRKCA reporter in H460 and A549 cells, but there was not affected in the luciferase activity of the MUT-circ-PRKCA reporter (Fig. 5C and D). Moreover, miR-384 was downregulated in NSCLC tissues and cells (Fig. 5E and F). Pearson's correlation analysis showed that miR-384 and circ-PRKCA expression had a negative correlation in NSCLC tissues (Fig. 5G). Also, the expression of circ-PRKCA was markedly lower in H460 and A549 cells after si-circ-PRKCA transfection compared to the control si-NC (Fig. 5H). Additionally, miR-384 expression was elevated in circ-PRKCA-inhibited H460 and A549 cells and was reduced in circ-PRKCA-increased H460 and A549 cells (Fig. 5I). These data manifested that circ-PRKCA acted as a sponge for miR-384 in NSCLC cells.

3.6. Inhibition of miR-384 overturned curcumin-mediated influence on the malignancy of NSCLC cells

Subsequently, we further explored whether curcumin regulated NSCLC cell malignancy by regulating miR-384 expression. After anti-miR-384 transfection, miR-384 expression was overtly reduced in H460 and A549 cells (Fig. 6A). Also, miR-384 silencing abrogated the elevation of miR-384 in H460 and A549 cells under curcumin treatment (Fig. 6B). Furthermore, miR-384 inhibition reversed the repressive role of curcumin on viability and colony formation of H460 and A549 cells (Fig. 6C and D). Moreover, the silence of miR-384 overturned the promotion of apoptosis of H460 and A549 cells mediated by curcumin treatment (Fig. 6E). Additionally, miR-384 inhibitor abolished the repressive effect of curcumin on migration and invasion of H460 and A549 cells (Fig. 6F and G). Together, these data manifested that curcumin regulated the malignancy of NSCLC cells via miR-384.

3.7. ITGB1 acted as a target for miR-384 in NSCLC cells

ITGB1 plays a promoting effect on NSCLC progression [20,21]. Herein, we performed western blotting analysis to verify impact of curcumin on ITGB1 protein level in NSCLC cells. The results exhibited that the level of ITGB1 protein was reduced in H460 and A549 cells with the elevation of curcumin (Fig. 7A). To explore the regulatory mechanism of miR-384 in NSCLC advancement, we predicted the targets of miR-384 by the starBase v2.0 database. As exhibited in Fig. 7B, ITGB1 possessed a complementary sequence to miR-384. Furthermore, the

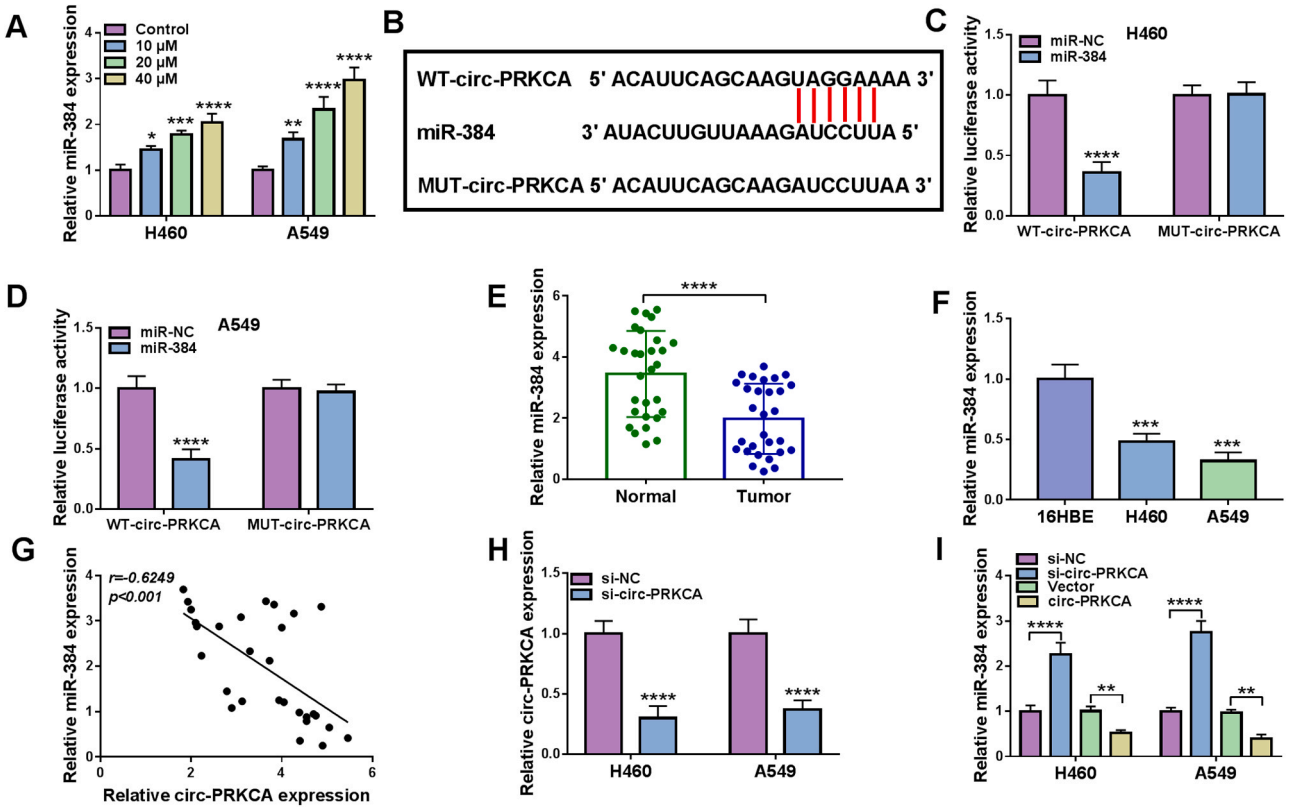

Fig. 5. Circ-PRKCA served as a sponge for miR-384 in NSCLC cells. (A) Effect of curcumin treatment on the expression of miR-384 in H460 and A549 cells was determined by qRT-PCR. (B) The sequence of circ-PRKCA possessed the complementary sites to miR-384. (C and D) Dual-luciferase reporter assay was executed to assess the luciferase activity in H460 and A549 cells co-transfected with miR-384 or miR-NC and WT-circ-PRKCA or MUT-circ-PRKCA reporter. (E and F) QRT-PCR was applied to analyze miR-384 expression in NSCLC tissues and cells (H460 and A549). (G) Assessment of the correlation between miR-384 and circ-PRKCA in NSCLC tissues by Pearson's correlation analysis. (H) After si-NC or si-circ-PRKCA transfection, the expression of circ-PRKCA was detected by qRT-PCR. (I) Influence of circ-PRKCA elevation and knockdown on miR-384 expression in H460 and A549 was evaluated by qRT-PCR. $^{**}P < 0.01$, $^{***}P < 0.001$, and $^{****}P < 0.0001$.

luciferase activity in H460 and A549 cells was decreased by co-transfecting with miR-384 mimic and ITGB1 3′UTR-WT reporter, but there was no overt change in H460 and A549 cells co-transfected with miR-384 mimic and ITGB1 3′UTR-MUT reporter (Fig. 7C and D). Compared to adjacent normal tissues, the levels of ITGB1 mRNA and protein were elevated in NSCLC tissues (Fig. 7E and F). Also, the level of

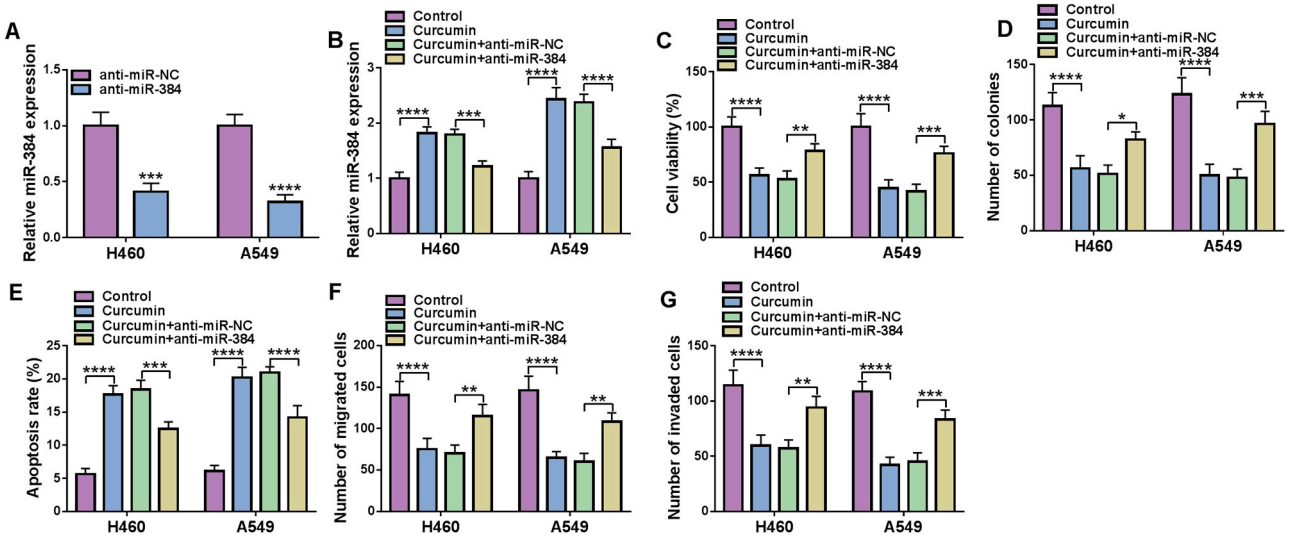

Fig. 6. Curcumin curbed the malignancy of NSCLC cells via elevating miR-384 expression. (A) The expression of miR-384 in H460 and A549 cells transfected with anti-miR-NC or anti-miR-384 was detected using qRT-PCR. (B) Expression of miR-384 in H460 and A549 cells transfected with anti-miR-NC or anti-miR-384 under curcumin treatment was measured by qRT-PCR. (C-G) Impacts of miR-384 inhibition on viability, colony formation, apoptosis, migration, and invasion of curcumin-treated H460 and A549 cells were determined using CCK-8, plate clone, flow cytometry, and transwell assays. $^{*}P < 0.05$, $^{**}P < 0.01$, $^{***}P < 0.001$, and $^{****}P < 0.0001$.

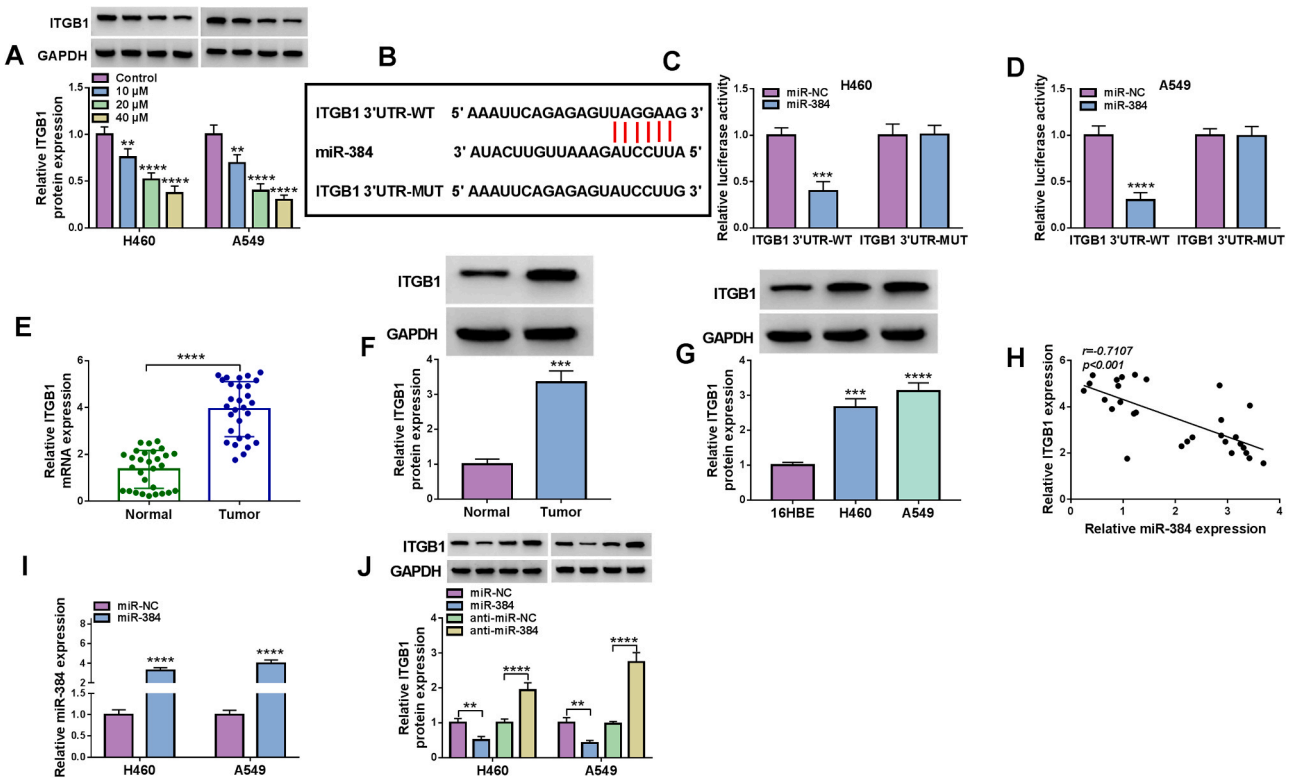

Fig. 7. ITGB1 served as a target for miR-384 in NSCLC cells. (A) Influence of curcumin treatment on the level of ITGB1 protein was assessed by western blotting. (B) The binding sites between miR-384 and ITGB1 were predicted by the starBase v2.0 database. (C and D) The binding sites between ITGB1 and miR-384 were verified by dual-luciferase reporter assay. (E and F) QRT-PCR and western blotting was performed to analyze the levels of ITGB1 mRNA and protein in NSCLC tissues and adjacent normal tissues. (G) Western blotting was executed to detect the level of ITGB1 protein in H460 and A549 cells and 16HBE cells. (H) Pearson's correlation analysis was used to determine the correlation between ITGB1 mRNA and miR-384 in NSCLC tissues. (I) QRT-PCR was conducted to verify the overexpression efficiency of miR-384 in H460 and A549 cells. (J) Influence of miR-384 overexpression and knockdown on the level of ITGB1 protein was analyzed by western blotting. $^{**}P < 0.01$, $^{***}P < 0.001$, and $^{****}P < 0.0001$.

ITGB1 protein was increased in H460 and A549 cells (Fig. 7G). There was a negative correlation between the expression of ITGB1 and miR-384 in NSCLC tissues (Fig. 7H). The overexpression efficiency of miR-384 was showed in Fig. 7I. Moreover, miR-384 overexpression decreased the level of ITGB1 protein in H460 and A549 cells, whereas miR-384 silencing had an opposing effect (Fig. 7J). Collectively, these

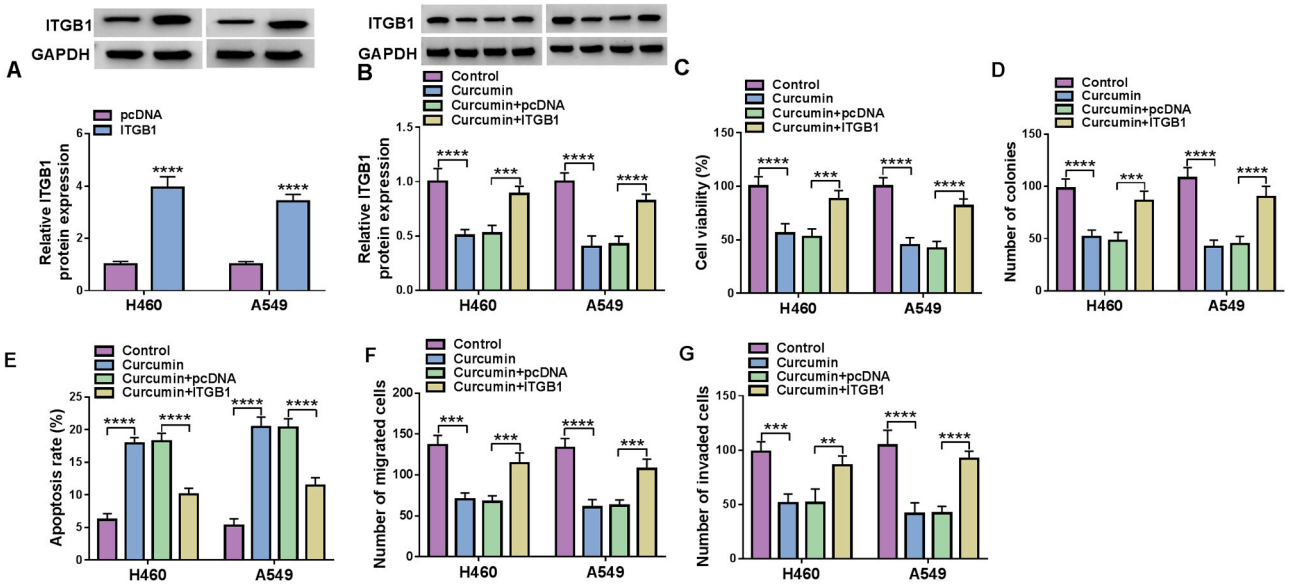

Fig. 8. Curcumin regulated the malignancy of NSCLC cells through ITGB1. (A) After pcDNA or ITGB1 transfection, the level of ITGB1 protein was examined using western blotting. (B) Influence of ITGB1 elevation on the level of ITGB1 protein in curcumin-treated H460 and A549 cells was determined by western blotting. (C-G) Effects of ITGB1 elevation on the viability, colony formation, apoptosis, migration, and invasion of curcumin-treated H460 and A549 cells were evaluated by CCK-8, plate clone, flow cytometry, and transwell assays. $^{**}P < 0.01$, $^{***}P < 0.001$, and $^{****}P < 0.0001$.

findings indicated that ITGB1 was a downstream target of miR-384 in NSCLC cells.

3.8. ITGB1 elevation reversed curcumin-mediated influence on the malignancy of NSCLC cells

In view of the above findings, we analyzed the impacts of ITGB1 overexpression on the malignancy of NSCLC cells mediated by curcumin treatment. The level of ITGB1 protein was apparently elevated in H460 and A549 cells after ITGB1 transfection (Fig. 8A). Moreover, ITGB1 overexpression overturned the downregulation of ITGB1 protein in curcumin-treated H460 and A549 cells (Fig. 8B). We also observed that the forcing expression of ITGB1 reversed the inhibitory impact of curcumin treatment on viability and colony formation of H460 and A549 cells (Fig. 8C and D). Furthermore, curcumin treatment elevated apoptosis and reduced migration and invasion of H460 and A549 cells, but these impacts were abolished after ITGB1 elevation (Fig. 8E-G). These results indicated that curcumin reduced the malignancy of NSCLC cells by downregulating ITGB1.

3.9. Curcumin regulated the malignancy of NSCLC cells by the circ-PRKCA/miR-384/ITGB1 pathway

Based on the above results, we further investigated whether curcumin regulated the malignancy of NSCLC cells by the circ-PRKCA/miR-384/ITGB1 axis. The results exhibited that circ-PRKCA inhibition reduced the level of ITGB1 protein in H460 and A549 cells, but this tendency was reversed after miR-384 inhibition (Fig. 9A). Moreover, circ-PRKCA overexpression partly overturned the decrease of ITGB1 protein in H460 and A549 cells under curcumin treatment (Fig. 9B). Also, silenced miR-384 expression abolished the repressive influence of curcumin on the level of ITGB1 protein in H460 and A549 cells (Fig. 9C). Collectively, these data indicated that curcumin-mediated circ-PRKCA sponged miR-384 to modulate ITGB1 expression in NSCLC cells.

4. Discussion

Curcumin has attracted the attention of scientific researchers all over the world because of its anti-cancer potential. Accumulated studies have revealed that curcumin can target cell signaling pathways related to cancer development [22]. For example, curcumin elevated miR-99a expression in retinoblastoma cells, thereby blocking the JAK/STAT pathway and repressed cell malignancy [23]. Moreover, curcumin inhibited the proliferation of glioblastoma cells via blocking the AKT/mTOR pathway [24]. Recent research revealed that curcumin elevated nasopharyngeal cancer radio-sensitization through regulating the circRNA/miR/mRNA network [10]. Herein, we discovered that curcumin curbed the malignancy of NSCLC cells through repressing the circ-PRKCA/miR-384/ITGB1 pathway.

It is well known that PRKCA acted as an oncogene in diverse cancers. Previous research revealed that PLCE1 facilitated cell invasion and migration through increasing PRKCA expression and activating NF-κB signaling in esophageal cancer cells [25]. Zhang et al. indicated that the upregulation of PRKCA was associated with the poor prognosis of NSCLC patients with radio-therapy [26]. Circ-PRKCA is located at chr17:64728805-64738878, and its gene symbol is PRKCA. Report of Chen et al. discovered that circ-PRKCA knockdown repressed the tumorigenesis of NSCLC through inactivating p38/MAPK signaling through adsorbing miR-545-3p [17]. Herein, circ-PRKCA was validated to be upregulated in NSCLC tissues and cells. Moreover, curcumin reduced circ-PRKCA expression in NSCLC cells. Also, circ-PRKCA upregulation partly reversed the inhibitory impact of curcumin on cell malignancy in NSCLC cells. Furthermore, circ-PRKCA silencing reinforced the inhibitory influence of curcumin on xenograft tumor growth. Thus,

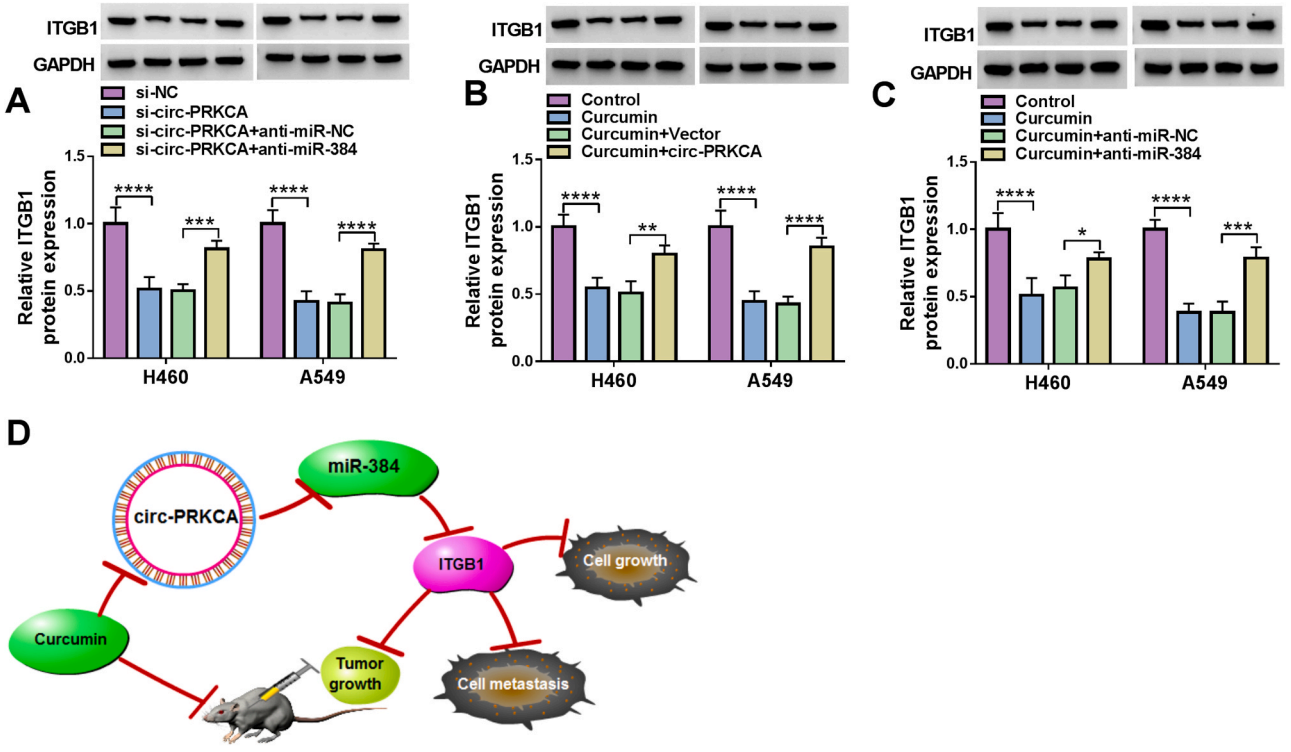

Fig. 9. Circ-PRKCA regulated ITGB1 expression by sponging miR-384 in curcumin-treated NSCLC cells. (A) The level of ITGB1 protein in H460 and A549 cells transfected with si-NC, si-circ-PRKCA, si-circ-PRKCA+anti-miR-NC, or si-circ-PRKCA+anti-miR-384 was detected using western blotting. (B and C) The level of ITGB1 protein in H460 and A549 cells transfected with Vector, circ-PRKCA, anti-miR-NC, or anti-miR-384 under curcumin treatment was analyzed using western blotting. (D) Schematic diagram of the mechanism by which curcumin inhibited the progression of NSCLC through the circ-PRKCA/miR-384/ITGB1 axis. $^{*}P < 0.05$, $^{**}P < 0.01$, $^{***}P < 0.001$, and $^{****}P < 0.0001$.

we inferred that curcumin repressed the malignancy of NSCLC cells at least in part through downregulation of circ-PRKCA.

Given that curcumin can increase the radio-sensitization of nasopharyngeal cancer through regulating the circRNA/miR/mRNA network [10]. We discovered that circ-PRKCA was a sponge of miR-384. Studies have marked that miR-384 plays a repressive role in a series of tumors, including osteosarcoma [27], breast cancer [28], colorectal cancer [29], and laryngeal cancer [30]. Inhibition of miR-384 contributed to metastasis and growth of osteosarcoma cells via decreasing SLBP expression [27]. Report of Wang et al. uncovered that lncRNA SNHG3 sponged miR-384 to elevate WEE1 expression, which accelerated migration and proliferation of laryngeal cancer cells [30]. Previous study reported that miR-384 impeded cell invasion and growth via targeting AEG-1 [31] and induced cell autophagy and apoptosis through downregulating COL10A [32] in NSCLC cells. Also, circRNA circ-0000376 sponged miR-384 to increase chemo-resistance, metastasis, and proliferation of NSCLC cells [33]. In the current study, miR-384 expression was elevated in curcumin-treated NSCLC cells. Moreover, miR-384 inhibitor partly overturned curcumin-mediated the malignancy of NSCLC cells. Therefore, curcumin regulated the malignancy of NSCLC cells by regulating the circ-PRKCA/miR-384 axis.

ITGB1 (CD29) is a member of the integrin family. It is comprised of 18α and 8β transmembrane subunits and interacts with extracellular matrix proteins to participate in cancer cell adhesion, survival, and metastasis [34]. Also, ITGB1 is a necessary factor in the vasculogenic mimicry of human cancer cells [35]. ITGB1 had been reported to be upregulated in diverse cancers, such as prostate cancer [36] and colorectal cancer [37]. Also, miR-424-5p [20] and miR-134 [38] decreased the growth of NSCLC through targeting ITGB1. Furthermore, lncRNA NR2F1-AS1 elevated ITGB1 expression by binding to miR-493–5p, thereby accelerating the malignant behaviors of NSCLC cells [21]. Herein, ITGB1 was validated as a target of miR-384. Moreover, curcumin repressed ITGB1 expression in NSCLC cells. The forcing expression of ITGB1 partly reversed curcumin-mediated the behaviors of NSCLC cells. What is more, curcumin-mediated circ-PRKCA regulated ITGB1 expression via sponging miR-384. Thus, we concluded that curcumin repressed the malignancy of NSCLC cells through the circ-PRKCA/miR-384/ITGB1 pathway (Fig. 9D). Given circRNAs and lncRNAs can act as miRNA sponges or molecular decoys, affecting the expression and activity of miRNAs, and then regulating the level of gene expression at the post-transcriptional level. Thus, we inferred that circRNAs and lncRNAs might jointly regulate IGTB1 expression by adsorbing different miRs, thereby regulating the progression of NSCLC. In sum, curcumin constrained the growth of NSCLC through down-regulating circ-PRKCA, which regulated ITGB1 expression by adsorbing miR-384. The research offered new evidence for the involvement of circRNA in curcumin-mediated NSCLC progression. Unfortunately, we did not verify the dose-dependent effect of curcumin in xenograft assays. This is a limitation of the manuscript and can be explored in the future.

Declarations

Ethics approval and consent to participate

The present study was approved by the ethical review committee of The Affiliated Hospital of Shandong University of TCM. Written informed consent was obtained from all enrolled patients.

Consent for publication

Patients agree to participate in this work.

Funding

No funding was received.

Conflict of interest statement

The authors declare that they have no competing interests.

Availability of data and materials

The analyzed data sets generated during the present study are available from the corresponding author on reasonable request.

Acknowledgement

Not applicable.

Appendix A. Supporting information

Supplementary data associated with this article can be found in the online version at doi:10.1016/j.biopha.2021.111439.

References

[1] X.-H. Jia, H. Xu, L.-Y. Geng, M. Jiao, W.-J. Wang, L.-L. Jiang, H. Guo, Efficacy and safety of neoadjuvant immunotherapy in resectable nonsmall cell lung cancer: a meta-analysis, Lung Cancer 147 (2020) 143–153.
[2] J. Wang, Z. Liu, Q. Pang, T. Zhang, X. Chen, P. Er, Y. Wang, P. Wang, J. Wang, Prognostic analysis of patients with non-small cell lung cancer harboring exon 19 or 21 mutation in the epidermal growth factor gene and brain metastases, BMC Cancer 20 (1) (2020) 837.
[3] L.A. Torre, R.L. Siegel, A. Jemal, Lung cancer statistics, Adv. Exp. Med. Biol. (2016) 1–19.
[4] Z. Wu, Z. Yang, Y. Dai, Q. Zhu, L.-A. Chen, Update on liquid biopsy in clinical management of non-small cell lung cancer, Onco Targets Ther. 12 (2019) 5097–5109.
[5] T. Tsuda, Curcumin as a functional food-derived factor: degradation products, metabolites, bioactivity, and future perspectives, Food Funct. 9 (2) (2018) 705–714.
[6] F.C. Rodrigues, N.V. Anil Kumar, G. Thakur, Developments in the anticancer activity of structurally modified curcumin: an up-to-date review, Eur. J. Med. Chem. 177 (2019) 76–104.
[7] L. Zhang, X. Tao, Q. Fu, C. Ge, R. Li, Z. Li, Y. Zhu, H. Tian, Q. Li, M. Liu, H. Hu, B. Zeng, Z. Lin, C. Li, R. Luo, X. Song, Curcumin inhibits cell proliferation and migration in NSCLC through a synergistic effect on the TLR4/MyD88 and EGFR pathways, Oncol. Rep. 42 (5) (2019) 1843–1855.
[8] Y. Pan, Y. Sun, Z. Liu, C. Zhang, miR-192–5p upregulation mediates the suppression of curcumin in human NSCLC cell proliferation, migration and invasion by targeting c-Myc and inactivating the Wnt/β-catenin signaling pathway, Mol. Med. Rep. 22 (2) (2020) 1594–1604.
[9] F. Liu, S. Gao, Y. Yang, X. Zhao, Y. Fan, W. Ma, D. Yang, A. Yang, Y. Yu, Antitumor activity of curcumin by modulation of apoptosis and autophagy in human lung cancer A549 cells through inhibiting PI3K/Akt/mTOR pathway, Oncol. Rep. 39 (3) (2018) 1523–1531.
[10] J. Yang, D. Zhu, S. Liu, M. Shao, Y. Liu, A. Li, Y. Lv, M. Huang, D. Lou, Q. Fan, Curcumin enhances radiosensitization of nasopharyngeal carcinoma by regulating circRNA network, Mol. Carcinog. 59 (2) (2020) 202–214.
[11] F. Wang, A.J. Nazarali, S. Ji, Circular RNAs as potential biomarkers for cancer diagnosis and therapy, Am. J. Cancer Res. 6 (6) (2016) 1167–1176.
[12] J.R. Welden, S. Stamm, Pre-mRNA structures forming circular RNAs, Biochim. Biophys. Acta Gene Regul. Mech. 1862 (11–12) (2019), 194410.
[13] X. Qi, D.H. Zhang, N. Wu, J.H. Xiao, X. Wang, W. Ma, ceRNA in cancer: possible functions and clinical implications, J. Med. Genet. 52 (10) (2015) 710–718.
[14] Z. Zhang, T. Yang, J. Xiao, Circular RNAs: promising biomarkers for human diseases, EBioMedicine 34 (2018) 267–274.
[15] K. Lei, H. Bai, Z. Wei, C. Xie, J. Wang, J. Li, Q. Chen, The mechanism and function of circular RNAs in human diseases, Exp. Cell Res. 368 (2) (2018) 147–158.
[16] J. Ding, Q. Wang, N. Guo, H. Wang, H. Chen, G. Ni, P. Li, CircRNA circ_0072995 promotes the progression of epithelial ovarian cancer by modulating miR-147a/CDK6 axis, Aging 12 (2020) 17209–17223.
[17] S. Chen, S. Lu, Y. Yao, J. Chen, G. Yang, L. Tu, Z. Zhang, J. Zhang, L. Chen, Downregulation of hsa_circ_0007580 inhibits non-small cell lung cancer tumorigenesis by reducing miR-545-3p sponging, Aging 12 (14) (2020) 14329–14340.
[18] Y. Li, Y. Zhang, S. Zhang, D. Huang, B. Li, G. Liang, Y. Wu, Q. Jiang, L. Li, C. Lin, Z. Wei, L. Meng, circRNA circARNT2 suppressed the sensitivity of hepatocellular carcinoma cells to cisplatin by targeting the miR-155-5p/PDK1 axis, Mol. Ther. Nucleic Acids 23 (2021) 244–254.
[19] S. Ganta, H. Devalapally, M. Amiji, Curcumin enhances oral bioavailability and anti-tumor therapeutic efficacy of paclitaxel upon administration in nanoemulsion formulation, J. Pharm. Sci. 99 (11) (2010) 4630–4641.
[20] Z.L. Xu, M. Zhang, S.X. Chen, M. Qiu, Q. Zhang, L.P. Gao, J.D.X. Li, MicroRNA-424-5p inhibits the development of non-small cell LCa by binding to ITGB1, Eur. Rev. Med. Pharmacol. Sci. 23 (20) (2019) 8921–8930.

[21] C. Zhang, S. Wu, R. Song, C. Liu, Long noncoding RNA NR2F1-AS1 promotes the malignancy of non-small cell lung cancer via sponging microRNA-493-5p and thereby increasing ITGB1 expression, Aging (2020) 12.
[22] A. Giordano, G. Tommonaro, Curcumin and cancer, Nutrients 11 (2019) 2376.
[23] Y. Li, W. Sun, N. Han, Y. Zou, D. Yin, Curcumin inhibits proliferation, migration, invasion and promotes apoptosis of retinoblastoma cell lines through modulation of miR-99a and JAK/STAT pathway, BMC Cancer 18 (1) (2018) 1230.
[24] Z. Wang, F. Liu, W. Liao, L. Yu, Z. Hu, M. Li, H. Xia, Curcumin suppresses glioblastoma cell proliferation by p-AKT/mTOR pathway and increases the PTEN expression, Arch. Biochem. Biophys. 689 (2020), 108412.
[25] Y. Li, C. Luan, Promotes the invasion and migration of esophageal cancer cells by up-regulating the PKCα/NF-κB pathway, Yonsei Med. J. 59 (10) (2018) 1159–1165.
[26] N. Zhang, Y. Song, Y. Xu, J. Liu, Y. Shen, L. Zhou, J. Yu, M. Yang, MED13L integrates mediator-regulated epigenetic control into lung cancer radiosensitivity, Theranostics 10 (20) (2020) 9378–9394.
[27] Y. Wang, H. Huang, Y. Li, Knocking down miR-384 promotes growth and metastasis of osteosarcoma MG63 cells by targeting SLBP, Artif. Cells Nanomed. Biotechnol. 47 (1) (2019) 1458–1465.
[28] Q. Ma, X. Qi, X. Lin, L. Li, L. Chen, W. Hu, LncRNA SNHG3 promotes cell proliferation andinvasion through the miR-384/hepatoma-derived growth factor axis in breastcancer, Hum Cell. 33 (1) (2020) 232–242.
[29] Y.X. Wang, H.F. Zhu, Z.Y. Zhang, F. Ren, Y.H. Hu, MiR-384 inhibits the proliferation of colorectal cancer by targeting AKT3, Cancer Cell Int. 18 (2018) 124.
[30] L. Wang, K. Su, H. Wu, J. Li, D. Song, LncRNA SNHG3 regulates laryngeal carcinoma proliferation and migration by modulating the miR-384/WEE1 axis, Life Sci. 232 (2019), 116597.
[31] N. Fan, J. Zhang, C. Cheng, X. Zhang, J. Feng, R. Kong, MicroRNA-384 represses the growth and invasion of non-small-cell lung cancer by targeting astrocyte elevated gene-1/Wnt signaling, Biomed. Pharmacol. 95 (2017) 1331–1337.
[32] Q. Guo, M. Zheng, Y. Xu, N. Wang, W. Zhao, MiR-384 induces apoptosis and autophagy of non-small cell lung cancer cells through the negative regulation of Collagen α-1(X) chain gene, Biosci. Rep. 39 (2019) 2.
[33] H. Sun, Y. Chen, Y.-Y. Fang, T.-Y. Cui, X. Qiao, C.-Y. Jiang, Z.-B. Lu, Circ_0000376 enhances the proliferation, metastasis, and chemoresistance of NSCLC cells via repressing miR-384, Cancer Biomark. 29 (2020) 463–473.
[34] L. Huang, X. Li, W. Gao, Long non-coding RNA linc-ITGB1 promotes cell proliferation, migration, and invasion in human hepatoma carcinoma by up-regulating ROCK1, Biosci. Rep. 38 (5) (2018).
[35] R. Kawahara, Y. Niwa, S. Simizu, Integrin β1 is an essential factor in vasculogenic mimicry of human cancer cells, Cancer Sci. 109 (8) (2018) 2490–2496.
[36] T. Pellinen, S. Blom, ITGB1-dependent upregulation of Caveolin-1 switches TGFβ signalling from tumour-suppressive to oncogenic in prostate cancer, Sci. Rep. 8 (1) (2018) 2338.
[37] M.A. Del Pozo, S. Laudato, N. Patil, M.L. Abba, J.H. Leupold, A. Benner, T. Gaiser, A. Marx, H. Allgayer, P53-induced miR-30e-5p inhibits colorectal cancer invasion and metastasis by targeting ITGA6 and ITGB1, Sci. Rep. 141 (9) (2017) 1879–1890.
[38] Q. Qin, F. Wei, J. Zhang, B. Li, miR-134 suppresses the migration and invasion of non-small cell lung cancer by targeting ITGB1, Oncol. Rep. 37 (2) (2017) 823–830.